# Aerosol Formation Yields from the Reaction of Catechol with Ozone

**ARTICLE** *in* ATMOSPHERIC ENVIRONMENT · MAY 2009

Impact Factor: 3.28 · DOI: 10.1016/j.atmosenv.2008.12.054

Atmospheric Environment 43 (2009) 2360–2365

Contents lists available at ScienceDirect

Atmospheric Environment

journal homepage: www.elsevier.com/locate/atmosenv

# Aerosol formation yields from the reaction of catechol with ozone

Cécile Coeur-Tourneur [a,*], Alexandre Tomas [b], Angélique Guilloteau [b,d], Françoise Henry [a], Frédéric Ledoux [a], Nicolas Visez [b], Véronique Riffault [b], John C. Wenger [c], Yuri Bedjanian [d]

[a] Laboratoire de Physico-Chimie de l'Atmosphère, UMR CNRS 8101, Université du Littoral Côte d'Opale, 32 avenue Foch, 62 930 Wimereux, France
[b] Département Chimie et Environnement, École des Mines de Douai, 941 rue Charles Bourseul, 59 508 Douai, France
[c] Department of Chemistry and Environmental Research Institute, University College Cork, Cork, Ireland
[d] Institut de Combustion, Aérothermique, Réactivité et Environnement, CNRS, 1C avenue de la Recherche Scientifique, 45 071 Orléans, France

ARTICLE INFO

*Article history:*
Received 22 July 2008
Received in revised form
21 November 2008
Accepted 24 December 2008

*Keywords:*
Catechol
Secondary organic aerosol yields
Smog chamber

ABSTRACT

The formation of secondary organic aerosol from the gas-phase reaction of catechol (1,2-dihydroxybenzene) with ozone has been studied in two smog chambers. Aerosol production was monitored using a scanning mobility particle sizer and loss of the precursor was determined by gas chromatography and infrared spectroscopy, whilst ozone concentrations were measured using a UV photometric analyzer. The overall organic aerosol yield ($Y$) was determined as the ratio of the suspended aerosol mass corrected for wall losses ($M_o$) to the total reacted catechol concentrations, assuming a particle density of 1.4 g cm$^{-3}$. Analysis of the data clearly shows that $Y$ is a strong function of $M_o$ and that secondary organic aerosol formation can be expressed by a one-product gas–particle partitioning absorption model. The aerosol formation is affected by the initial catechol concentration, which leads to aerosol yields ranging from 17% to 86%. The results of this work are compared to similar studies reported in the literature.



## 1. Introduction

Aromatic hydrocarbons are an important class of volatile organic compounds (VOCs) that are emitted into the troposphere as a result of anthropogenic activities (Piccot et al., 1992). Atmospheric oxidation of these hydrocarbons leads to the production of ozone as well as low-volatility species which can then partition into the condensed phase, forming secondary organic aerosol (SOA). The aromatics are believed to be a major anthropogenic source of SOA in urban areas (Seinfeld and Pandis, 1998). Despite considerable efforts over the last 10 years, the basic underlying mechanisms of secondary organic aerosol formation and growth from aromatic precursors remain poorly understood. Besides, the present knowledge on the formation of SOA is not able to explain the observed levels of SOA in the atmosphere, thus indicating that a large number of VOCs (especially those from anthropogenic sources) are currently not taken into account in the SOA-forming reactions included in the existing models (Volkamer et al., 2006; Weitkamp et al., 2007).

In the atmosphere, benzene and the alkyl substituted benzenes such as toluene, the xylenes and trimethylbenzenes react mainly with the hydroxyl radical (OH) during the day. In addition, reaction with the nitrate radical ($NO_3$) can contribute to their degradation mainly during the night. The reaction with OH leads to the formation of phenol, cresols and dimethylphenols in significant yields (up to 60%) from benzene, toluene and xylenes, respectively (Berndt and Böge, 2001; Klotz et al., 2002; Smith et al., 1999, 1998; Volkamer et al., 2002a,b). These monohydroxylated aromatic compounds react only slowly with $O_3$ (Calvert et al., 2002) and their reaction with OH and $NO_3$ radicals are rapid and result in phenol, cresol and dimethylphenol lifetimes in the troposphere which are significantly shorter than those of their parent aromatic hydrocarbons (Calvert et al., 2002). The reaction of benzene, phenol and cresols with OH has been shown to produce 1,2-benzenediols (also known as catechols) with high yields, around 80% (Berndt and Böge, 2003; Olariu et al., 2002).

The reactivity of 1,2-benzenediol compounds with $O_3$ is much higher than what is normally observed for the reaction of $O_3$ with alkylbenzenes, phenols and cresols (Calvert et al., 2002; Tomas et al., 2003). This is linked to the two neighboring OH groups that raise the electron density at these sites and facilitate reactivity toward electrophilic reagents like $O_3$. Interestingly, preliminary investigations performed at the European Photoreactor (EUPHORE), showed that the gas-phase reaction of catechol with ozone produced significant amounts of secondary organic aerosol (Olariu et al., 2003). Until recently, the formation of SOA from aromatic compounds has been mainly focused on the alkylbenzenes (Hu and Kamens, 2007; Hurley et al., 2001; Jang and Kamens,

* Corresponding author. Tel.: +33 321 99 64 05; fax: +33 321 99 64 01.
*E-mail address:* coeur@univ-littoral.fr (C. Coeur-Tourneur).

1352-2310/$ – see front matter © 2009 Elsevier Ltd. All rights reserved.
doi:10.1016/j.atmosenv.2008.12.054

2001; Johnson et al., 2005; Kleindienst et al., 1999; Martin-Reviejo and Wirtz, 2005; Ng et al., 2007; Odum et al., 1996, 1997b; Song et al., 2005, 2007a,b; Takekawa et al., 2003), with little attention paid to their oxidation products, although the formation of SOA from the OH initiated oxidation of the cresols was recently studied in our laboratory (Henry et al., 2008). In this work, we have investigated the formation of SOA from the reaction of ozone with catechol in two different smog chambers. SOA formation yields obtained in the two chambers have been compared and analyzed using the absorptive gas–particle partitioning model (Odum et al., 1996; Pankow, 1994a,b).

## 2. Experimental

The study was carried out using mainly the smog chamber at the Laboratoire de Physicochimie de l'Atmosphère of the Université du Littoral Côte d'Opale, France (LPCA – ULCO). Additional experiments were performed at the Centre for Research into Atmospheric Chemistry (CRAC), University College Cork, Ireland. The experimental facilities in these two laboratories provide complementary information concerning secondary organic aerosol formation during the ozone-initiated oxidation of catechol.

### 2.1. Smog chamber at the LPCA

Experiments at the LPCA were performed in a darkened 8 $m^3$ cubic evacuable Plexiglas reaction chamber, at atmospheric pressure, room temperature ($294 \pm 2$ K) and low relative humidity (5–10%). The gas mixture was continuously stirred by a fan at the bottom of the reactor, thus ensuring a homogeneous mixing of the reactants. The smog chamber has been described in detail elsewhere (Coeur-Tourneur et al., 2006).

The experimental procedure was as follows: first, ozone was introduced into the chamber by passing clean air through a mercury lamp $O_3$ generator (Thermo Environmental Instruments Inc. Dynamic Gas Calibration System – Model 146). Secondly a known volume of catechol dissolved into water (solution at 25%) was injected into the chamber after vaporization at 553 K. Its introduction corresponded to the beginning of the reaction. Chemicals used and their purity levels were as follows: catechol >99% (Merck products). All experiments were carried out in the absence of inorganic seed aerosol and were conducted until the suspended aerosol mass (corrected for wall losses) $M_o$ was constant (corresponding to approximately 6 h of reaction).

The loss of reactants and formation of aerosol was monitored throughout the experiments. The catechol concentration was determined by gas-chromatography with flame ionisation detection (Perkin Elmer, Turbomatrix-GC-FID). The catechol was collected at room temperature, onto stainless steel tubes filled with Tenax TA (60–80 mesh) and thermally desorbed onto a 30 m DB-5 Megabore fused silica capillary column held at 313 K for 5 min and then programmed to 523 K at 5 K $min^{-1}$. Ozone concentrations were measured by a UV photometric analyzer (Thermo Electron Corporation $O_3$ Analyzer – Model 49C). Particle size distributions (in the 11–1083 nm diameter range) and concentrations were monitored with a Scanning Mobility Particle Sizer (SMPS, GRIMM, CPC 5.404). The SMPS sampled every 6 min with a 1 min delay between samples. The aerosol mass formed during the reaction time was obtained from the aerosol volume concentration assuming a density of 1.4 g $cm^{-3}$ for the organic aerosol, which has been shown by Bahreini et al. (2005) to be a reasonable approximation.

Reactor walls could be a source of gas and/or particles, due to either the offgasing of compounds that react to form SOA or the direct release of particles. Moreover, the impurities in the air of the chamber can also react with ozone to form SOA. As a result, a number of preliminary experiments and tests were performed in the smog chamber. Before an experimental run, the chamber was flushed for 24 h with purified air produced by a pure air generator (Dominick Hunter LGCAD 140). The amount of particles in the background air was determined by SMPS to be very small, with typical particle number concentrations less than 10 $cm^{-3}$. Controlled experiments in which ozone and purified air were mixed for 6 h were performed. The aerosol mass concentration determined in these tests was lower than 3 μg $m^{-3}$, with a mean diameter of about 50 nm. This background is negligible compared to the SOA mass formed during the ozone reaction with catechol.

The aerosol concentration was determined from the measured values corrected for aerosol deposition on the walls of the chamber. Wall losses are described by a first order law, with a dependence on the aerosol size. The deposition rates of secondary organic aerosol were measured in the dark by observing the decay of the aerosol concentration at the end of the experiments after addition of NO to destroy $O_3$. The deposition rate constants determined in this work were about 3–4% $h^{-1}$ for the LPCA chamber. These values are within the range reported for other large chamber facilities (Henry et al., 2008; Hurley et al., 2001; Takekawa et al., 2003).

Catechol wall loss rates of about 8–9% $h^{-1}$ were also determined in the dark over a period of 6 h. Corrections for wall losses were applied to both catechol and SOA data.

### 2.2. Smog chamber at the CRAC

Complementary experiments were performed at the CRAC chamber which is a cylindrical 3.9 $m^3$ reactor made of FEP foil operated at atmospheric pressure, room temperature ($295 \pm 2$ K) and low relative humidity (0.03–3%). Only the main features of the experimental set-up will be provided here; a more detailed description can be found elsewhere (Thüner et al., 2004).

Prior to the addition of reactants, the chamber was flushed with purified air for at least 4 h at 150 L $min^{-1}$ and analysis of the contents was carried out to ensure that no impurities (hydrocarbons, $NO_x$ or particles) were present. Weighed amounts of catechol were introduced in the chamber via a small air flow by using a heated impinger. Around 30 min was allowed for the catechol to reach a stable concentration inside the reactor, as no mixing fans were present at the time of the experiments. Wall loss rates were determined for the next 30 min and ranged from 14 to 34% $h^{-1}$ in the different experiments. Ozone was then injected and started immediately to react with catechol. Reactant concentrations were monitored by *in situ* FTIR spectroscopy (BioRad spectrometer, 1 $cm^{-1}$ resolution, coupled to a 229.6 m long White cell) using integrated band intensities between 1112 and 1653 $cm^{-1}$ for catechol and the absorption cross-section at 1055 $cm^{-1}$ for ozone ($\sigma = 2 \times 10^{-20}$ $cm^2$ $molecule^{-1}$) (Olariu, 2001). Aerosol size distributions and particle numbers were determined by a TSI 3080 Scanning Mobility Particle Sizer (SMPS) with a time resolution of 3 min. Aerosol wall losses were determined at the end of the reaction and allowed for the correction of the organic aerosol mass formed. The aerosol wall loss rate was typically 72% $h^{-1}$.

## 3. Results and discussion

### 3.1. Aerosol formation profiles

A series of seven experiments were conducted at the LPCA and three at the CRAC. The experimental conditions are reported in Table 1. Initial concentrations of catechol and ozone varied significantly, from 61 to 1293 ppbV and from 102 to 1400 ppbV, respectively. In the case of the first two CRAC experiments, large

**Table 1**
Initial conditions for the experiments performed in the LPCA and CRAC smog chambers.

| Expt. | [catechol]$_o$[a] | | [ozone]$_o$[b] | | OH scavenger[c] |
|---|---|---|---|---|---|
| | ppbV | μg m$^{-3}$ | ppbV | μg m$^{-3}$ | % |
| LPCA | | | | | |
| LPCA-1 | 897 | 4112 | 374 | 748 | – |
| LPCA-2 | 669 | 3066 | 102 | 204 | – |
| LPCA-3 | 646 | 2960 | 340 | 680 | – |
| LPCA-4 | 320 | 1468 | 250 | 500 | – |
| LPCA-5 | 280 | 1283 | 200 | 400 | – |
| LPCA-6 | 160 | 735 | 201 | 402 | – |
| LPCA-7 | 61 | 281 | 206 | 412 | – |
| CRAC | | | | | |
| CRAC-1 | 742 | 3399 | 1400 | 2800 | 2.5 |
| CRAC-2 | 219 | 1004 | 498 | 996 | 2.5 |
| CRAC-3 | 1293 | 5926 | 610 | 1220 | – |

[a] Initial catechol concentrations.
[b] Initial ozone concentrations. For the CRAC experiments, ozone was undergoing reaction with catechol as it was being added to the chamber. The value corresponds to the maximum observed concentration.
[c] CO was used as OH scavenger in the experiments performed at the CRAC. No scavenger was used at LPCA.

amounts of CO (2.5%) were added to scavenge the OH radicals which could be formed from the catechol ozonolysis.

Fig. 1 shows typical concentration-time profiles obtained at the LPCA for catechol, $O_3$ and the measured aerosol mass (experiment LPCA-5). The corresponding time-series of aerosol size distributions is shown in Fig. 2. Similar plots were obtained at CRAC. In all the experiments SOA formation was observed immediately after the addition of the second reactant (*i.e.* catechol for the LPCA experiments, ozone for the CRAC experiments). In the first few minutes there was a very fast increase in the particle number concentration followed by a gradual decrease throughout the experiment. This observation is consistent with an initial nucleation step producing a burst of nano-particles, followed by coagulation of these particles which results in an increase in the mean particle size, along with a corresponding decrease in the number. The initial particles observed were fairly small, with mean diameters starting at about 90 nm for the smallest initial reactant

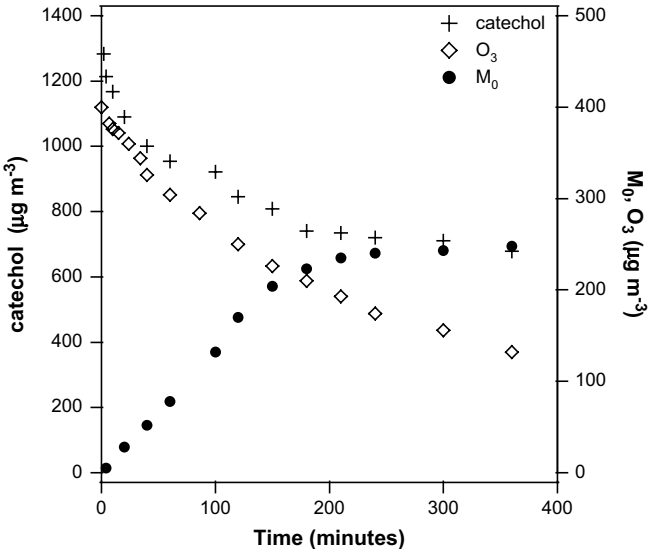


**Fig. 1.** Reaction-time profile of a typical photooxidation experiment (LPCA-5, initial conditions: 1283 μg m$^{-3}$ catechol and 400 μg m$^{-3}$ ozone).

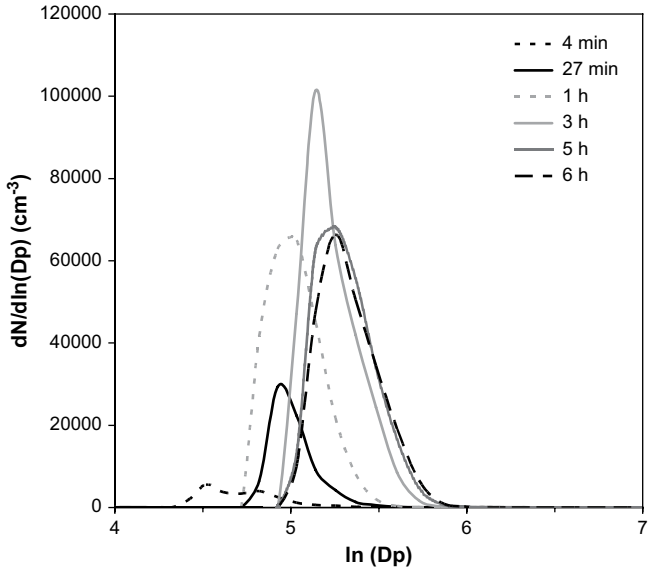


**Fig. 2.** Aerosol size distributions of a typical photooxidation experiment (experiment LPCA-5, initial conditions: 1283 μg m$^{-3}$ catechol and 400 μg m$^{-3}$ ozone).

concentrations. Rapid growth led to particles with a final mean diameter of around 190 nm.

Two plots of the organic aerosol mass formed ($M_o$) as a function of the catechol mass reacted (Δ[cat]) are provided in Fig. 3, corresponding to experiments LPCA-5 and CRAC-1. These plots reveal that an initial amount of reacted catechol is required before the rise of the aerosol mass is measured. This reacted amount is about 160–300 μg m$^{-3}$, depending on the initial catechol and ozone concentrations.

Time-dependent growth curves of aerosol mass versus hydrocarbon consumption have been plotted by Ng et al. (2006) in their study of the ozonolysis of ten biogenic hydrocarbons with at least one double bond. Most experiments were performed in low-RH ammonium sulfate seeded conditions and for ozone concentrations largely exceeding (about three times) those of the hydrocarbon. Two different types of curves have been established: (i) compounds with one double bond mainly exhibiting a linear growth in aerosol mass after the initiation period and (ii) compounds with at least two double bonds presenting a linear growth followed by a curve region where no hydrocarbon consumption is observed and yet the SOA mass is still increasing. A possible explanation discussed by Ng et al. (2006) is that SOA formation in these later stages is due to further oxidation of the unsaturated first-generation products. In our study three experiments have been carried out where the ozone concentration is in excess, by a factor of 2–3 (LPCA-7, CRAC-1, and CRAC-2). A typical growth curve for this case (CRAC-1 experiment) is shown in Fig. 3b. The last part of the plot clearly shows that the aerosol mass continues to accumulate whilst the catechol reactivity has stopped, which seems to indicate the further oxidation by $O_3$ of gaseous unsaturated products leading to semi-volatile compounds. In the only previous study of SOA formation from the reaction of catechol with ozone, performed at EUPHORE (Olariu et al., 2003), one experiment was carried out in excess of ozone (EUPHORE-5), but the observed growth in aerosol mass was solely linear. However, less than 20% of catechol was consumed in this particular experiment, providing little opportunity for any secondary chemistry to contribute to SOA formation.

Fig. 3b suggests that the SOA formation from the reaction of catechol with $O_3$ appears to result from two sources: (i) the

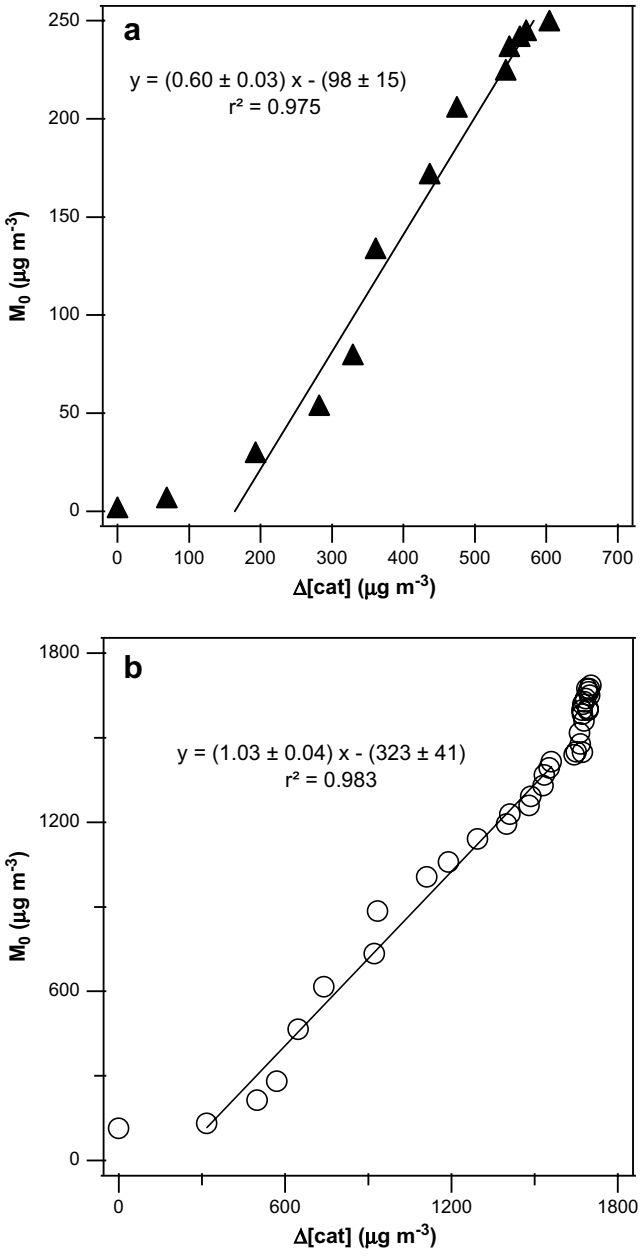


**Fig. 3.** Plots of the SOA mass concentration ($M_o$) against the reacted catechol concentration (Δ[cat]). (a): experiment LPCA-5 (the straight line represents a linear regression on all the data points except the first two); (b): experiment CRAC-1 (the straight line represents a linear regression on the data points for Δ[cat] = (300–1600) µg m$^{-3}$).

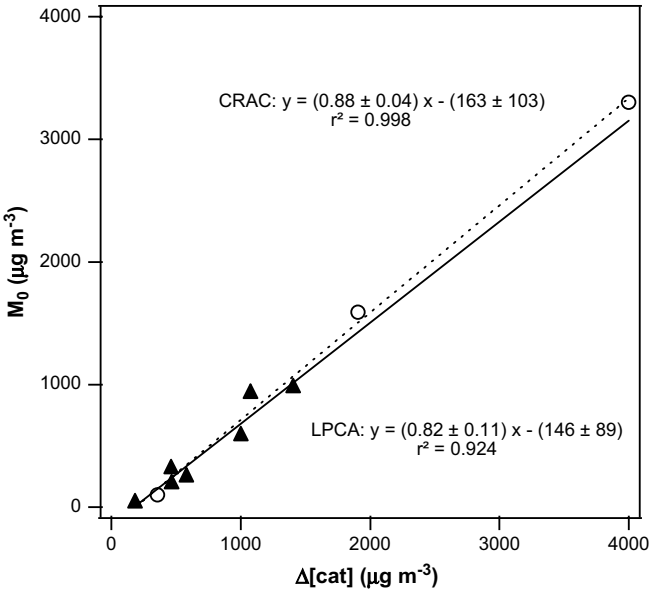


**Fig. 4.** Plot of the SOA mass concentration against the reacted catechol concentration measured at the end of the experiments. Each data point represents a separate experiment. LPCA (▲); CRAC (○).

primary reaction after the saturation vapour pressure of the products is reached and (ii) further reaction of the first generation products, possibly quinones or ring opening products.

Fig. 4 presents the plot of the SOA mass concentration ($M_o$) against the reacted catechol concentration (Δ[cat]) at the end of each experiment. This figure shows strong linear correlations for the LPCA ($R^2 = 0.92$) and CRAC data ($R^2 = 0.99$), with slopes of 0.82 and 0.88 respectively. These values correspond to the highest aerosol yields determined in both smog chambers. This figure also displays that the aerosol mass produced in the smog chamber starts to be substantial after a certain amount (about 180 µg m$^{-3}$) of the reacting organic gas has been oxidized. This value is in accordance with those observed in the individual experiments in LPCA and CRAC (Fig. 3).

### 3.2. SOA yield parameters

SOA yields ($Y$) can be determined experimentally by calculating the ratio of the organic aerosol mass concentration $M_o$ (in µg m$^{-3}$) to the amount of catechol reacted Δ[cat] at the end of each experiment:

$$Y = \frac{M_o}{\Delta[\text{cat}]} \quad (1)$$

SOA yields can also be described by a semi-empirical model based on absorptive gas–particle partitioning of semi-volatile products (Odum et al., 1996; Pankow, 1994a,b):

$$Y = \sum_i M_o \frac{\alpha_i K_{om,i}}{1 + K_{om,i} M_o} \quad (2)$$

in which $\alpha_i$ is the mass-based gas-phase stoichiometric fraction for semi-volatile species $i$ and $K_{om,i}$ is the gas–particle partitioning coefficient for species $i$. This equation can be used to fit the experimental yield data and determine values for $\alpha_i$ and $K_{om,i}$,. Fig. 5 displays the SOA yield versus the concentration of organic aerosol $M_o$ formed from the ozone + catechol reaction in the LPCA and CRAC chambers. The data from the EUPHORE chamber experiments (Olariu et al., 2003) are included for comparison. The simulation of all the data $Y = f(M_o)$ from the present experimental study demonstrates that a one-product model is able to accurately reproduce the data; the use of two or more products in the model did not improve the quality of the fits. The following SOA yield parameters have been determined: $\alpha = 0.91 \pm 0.15$ and $K_{om} = (4.8 \pm 2.9) \times 10^{-3}$ m$^3$ µg$^{-1}$ at the 95% confidence level. It is interesting to note that when considering only the LPCA data, values of $\alpha$ and $K_{om}$ remain the same and only the corresponding uncertainties increase by a factor of 2.5. Many studies on SOA yields from aromatic compounds have reported that the aerosol yield data should be fitted assuming two hypothetical products (Odum et al.,

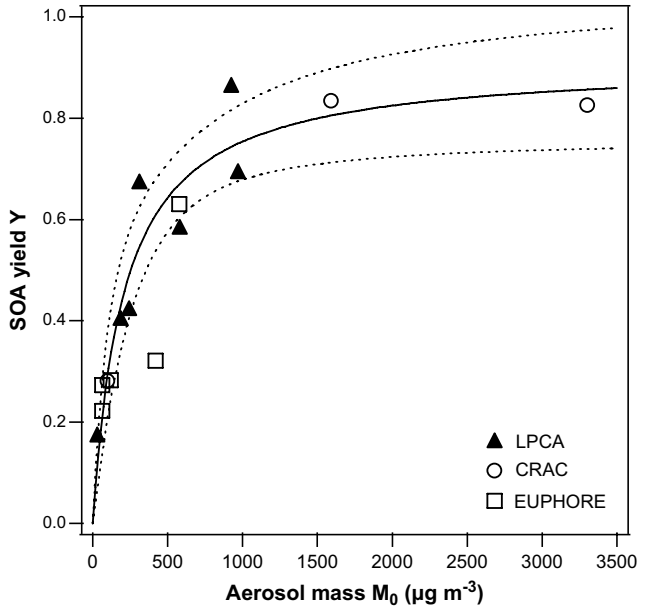


**Fig. 5.** Aerosol yield ($Y$) as a function of the organic aerosol mass formed ($M_o$). LPCA (▲), CRAC (○) and EUPHORE (□) (Olariu et al., 2003). The solid line represents the best fit to the LPCA and CRAC data considering one semi-volatile major product ($\alpha = 0.91$; $K_{om} = 4.8 \times 10^{-3}\ m^3\ \mu g^{-1}$). The dotted lines represent the upper and lower limits for the 95% confidence interval.

**Table 2**
Experimental results obtained in the LPCA and CRAC smog chambers; EUPHORE data from Olariu et al. (2003) have been added for comparison.

| Expt. | Δ[cat][a] | | | Δ[ozone][b] | | | $M_o$[c] | Y[d] |
|---|---|---|---|---|---|---|---|---|
| | ppbV | µg m$^{-3}$ | % | ppbV | µg m$^{-3}$ | % | µg m$^{-3}$ | % |
| LPCA – This work | | | | | | | | |
| LPCA-1 | 235 | 1076 | 26 | 281 | 562 | 75 | 925 | 86 |
| LPCA-2 | 101 | 463 | 15 | 47 | 94 | 46 | 310 | 67 |
| LPCA-3 | 307 | 1406 | 47 | 222 | 444 | 65 | 970 | 69 |
| LPCA-4 | 218 | 1000 | 68 | 138 | 276 | 55 | 580 | 58 |
| LPCA-5 | 126 | 579 | 45 | 113 | 226 | 57 | 243 | 42 |
| LPCA-6 | 101 | 465 | 63 | 116 | 332 | 58 | 186 | 40 |
| LPCA-7 | 40 | 182 | 65 | 76 | 152 | 37 | 31 | 17 |
| CRAC – This work | | | | | | | | |
| CRAC-1 | 416 | 1906 | 56 | 1000 | 2000 | 71 | 1590 | 83 |
| CRAC-2 | 78 | 356 | 35 | 200 | 400 | 40 | 100 | 28 |
| CRAC-3 | 873 | 4000 | 67 | 200 | 400 | 33 | 3302 | 83 |
| EUPHORE – Olariu et al. (2003) | | | | | | | | |
| EUPHORE-1 | 285 | 1308 | 21 | n.a. | – | – | 419 | 32 |
| EUPHORE-2 | 61 | 279 | 20 | n.a. | – | – | 62 | 22 |
| EUPHORE-3 | 92 | 422 | 30 | n.a. | – | – | 119 | 28 |
| EUPHORE-4 | 267 | 1084 | 85 | n.a. | – | – | 770 | 63 |
| EUPHORE-5 | 50 | 229 | 17 | n.a. | – | – | 63 | 27 |

[a] Reacted catechol concentrations.
[b] Reacted ozone concentrations. CRAC values are estimated as ozone already started to react before reaching its maximum concentration. EUPHORE data were not available (n.a.).
[c] Organic aerosol mass concentration (corrected for wall losses and assuming a particle density of 1.4 g cm$^{-3}$).
[d] SOA yield calculated as the ratio of $M_o$ to the total reacted catechol concentration.

1997a,b; Song et al., 2005). However, a number of recent studies have shown that the organic aerosol yield formed in aromatic photooxidation systems could be well described by assuming only one hypothetical product (Ferri et al., 2001; Henry et al., 2008; Olariu et al., 2001; Takekawa et al., 2003). Although the organic aerosol phase is often composed of many oxidation products (Forstner et al., 1997), the present simulation with the one-product model indicates either that one semi-volatile organic compound is the major component of the condensed phase or that the few organics composing the SOA phase have similar $\alpha$ and $K_{om}$ values. In this latter case, the obtained constants $\alpha$ and $K_{om}$ would not have any intrinsic physical meaning but would rather represent mean values.

It is noteworthy that the value of $\alpha$ (0.91) is very close to that of the slope on Fig. 4 ($\sim$0.85) which corresponds to the highest aerosol yields determined in both smog chambers. Considering that $Y$ is the SOA yield (for the particle phase) and $\alpha$ is the stoichiometric fraction for all semi-volatile species ($\alpha$ takes into account compounds formed in the gas and aerosol phases), this suggests that the low-volatile compounds formed in the reaction of catechol with ozone are transferred almost completely into the particle phase. The same observations have been made for the catechol + $O_3$ (Olariu et al., 2003) and cresol + OH reactions (Henry et al., 2008).

As shown in Figs. 4 and 5, a fairly good agreement was observed between the two sets of experiments performed under different conditions in the LPCA and the CRAC smog chambers.

In the CRAC chamber, two experiments were conducted with CO as OH scavenger. The SOA formation yields determined from these two data sets displayed values which can be fit very well with those without OH scavenger. This indicates that either the OH radical production is not significant in the catechol ozonolysis or that the OH reaction with catechol leads to similar SOA yields than the one with ozone. In previous experiments performed at EUPHORE, Olariu et al. (2003) have shown OH formation from catechol ozonolysis and they have observed slightly higher aerosol yields without OH radical scavenger (with cyclohexane used as OH scavenger).

A summary of experimental results obtained in the experiments performed in the two chambers is provided in Table 2. The results reported from experiments performed in the EUPHORE chamber have also been included for comparative purposes. SOA yields obtained in the EUPHORE experiments have been recalculated using a particle density of 1.4 g cm$^{-3}$. There is good agreement between the 3 sets of data (except one EUPHORE experimental run) even though the chamber volume, reaction conditions and analytical techniques were somewhat different in each case.

## 4. Summary and conclusions

The ozonolysis of catechol has been investigated in environmental smog chamber experiments and has been shown to produce large amounts of secondary organic aerosol. The aerosol yields have been measured under $NO_x$-free, low-RH, and non-seeded conditions and values as high as 86% have been obtained. Therefore, the reaction of $O_3$ with catechol (and probably its methylated counterparts, Olariu et al., 2003) could contribute significantly to the aerosol loading of the lower troposphere in polluted areas, where ozone concentrations could be high. A one-product gas–particle partitioning absorption model has been successfully applied to explain SOA formation. Further investigation of the composition of both the gas and particulate phases would be necessary to identify the possible intermediates and supply data to model multiple oxidation steps leading to SOA formation.

## Acknowledgements

The LPCA and EMD participate in the Research Institute of Industrial Environment (IRENI) which is financed by the

Communauté Urbaine de Dunkerque, the Nord-Pas de Calais Regional Council, the French Ministry of Education and Research, and European funds (FEDER). Funding has also been received from the National Program "LEFE-CHAT". N. Visez wishes to thank ARMINES and the Ecole des Mines de Douai for his postdoctoral fellowship. A. Guilloteau gratefully acknowledges financial support from the European Science Foundation programme INTROP in the form of an exchange grant.

## References

Bahreini, R., Keywood, M.D., Ng, N.L., Varutbangkul, V., Gas, S., Flagan, R.C., Seinfeld, J.H., Worsnop, D.R., Jimenez, J.L., 2005. Measurements of secondary organic aerosol from oxidation of cycloalkenes, terpenes, and m-xylene using an aerodyne aerosol mass spectrometer. Environmental Science and Technology 39, 5674–5688.

Berndt, T., Böge, O., 2001. Gas-phase reaction of OH radicals with benzene: products and mechanism. Physical Chemistry Chemical Physics 3, 4946–4959.

Berndt, T., Böge, O., 2003. Gas-phase reaction of OH radicals with phenol. Physical Chemistry Chemical Physics 5, 342–350.

Calvert, J.G., Atkinson, R., Becker, H., Kamens, R.M., Seinfeld, J.H., Wallington, T.J., Yarwood, G., 2002. Mechanisms of Atmospheric Oxidation of Aromatic Hydrocarbons. Oxford University Press, New-York.

Coeur-Tourneur, C., Henry, F., Janquin, M.-A., Brutier, L., 2006. Gas-phase reaction of hydroxyl radicals with *m*-, *o*- and *p*-cresol. International Journal of Chemical Kinetics 38, 553–562.

Ferri, D., Astorga, C., Tedeschi, R., Winterhalter, R., Viidanoja, J., Bolzacchin,i E., Jensen, N.R., Larsen, B.R., Hjorth, J., 2001. Photo-oxidation of benzene, toluene and benzaldehyde: identification and quantification of reaction products in the gas-phase and in particles, In: Eighth European Symposium on the Physico-Chemical Behaviour of Atmospheric Pollutants, Torino, Italia, 17–20 September 2001.

Forstner, H.J.L., Flagan, R.C., Seinfeld, J.H., 1997. Molecular speciation of secondary organic aerosol from photooxidation of the higher alkenes: 1-octene and 1-decene. Atmospheric Environment 31, 1953–1964.

Henry, F., Coeur-Tourneur, C., Ledoux, F., Tomas, A., Menu, D., 2008. Secondary organic aerosol formation from the gas phase reaction of hydroxyl radicals with m-, o- and p-cresol. Atmospheric Environment 42, 3035–3045.

Hu, D., Kamens, R.M., 2007. Evaluation of the UNC toluene-SOA mechanism with respect to other chamber studies and key model parameters. Atmospheric Environment 41, 6465–6477.

Hurley, M.D., Sokolov, O., Wallington, T.J., Takekawa, H., Karasawa, M., Klotz, B., Barnes, I., Becker, K.H., 2001. Organic aerosol formation during the atmospheric degradation of toluene. Environmental Science and Technology 35, 1358–1366.

Jang, M., Kamens, R., 2001. Characterization of secondary aerosol from the photo-oxidation of toluene in the presence of $NO_x$ and 1-propene. Environmental Science and Technology 35, 3626–3639.

Johnson, D., Jenkin, M.E., Wirtz, K., Martin-Reviejo, M., 2005. Simulating the formation of secondary organic aerosol from the phootoxidation of aromatic hydrocarbons. Environmental Chemistry 2, 35–48.

Kleindienst, T.E., Smith, D.F., Edney, E.O., Driscoll, D.J., Speer, R.E., Weathers, W.S., 1999. Secondary organic aerosol formation from the oxidation of aromatic hydrocarbons in the presence of dry submicron ammonium sulfate aerosol. Atmospheric Environment 33, 3669–3681.

Klotz, B., Volkamer, R., Hurley, M.D., Andersen, M.P.S., Nielsen, O.J., Barnes, I., Imamura, T., Wirtz, K., Becker, K.H., Platt, U., Wallington, T.J., Washida, N., 2002. OH-initiated oxidation of benzene Part II. Influence of elevated $NO_x$ concentrations. Physical Chemistry Chemical Physics 4, 4399–4411.

Martin-Reviejo, M., Wirtz, K., 2005. Is benzene a precursor for secondary organic aerosol? Environmental Science and Technology 39, 1045–1054.

Ng, N.L., Kroll, J.H., Keywood, M.D., Bahreini, R., Varutbangkul, V., Flagan, R.C., Seinfeld, J.H., Lee, A., Goldstein, A.H., 2006. Contribution of first- versus second-generation products to secondary organic aerosols formed in the oxidation of biogenic hydrocarbons. Environmental Science and Technology 40, 2283–2297.

Ng, N.L., Kroll, J.H., Chan, A.W.H., Chhabra, P.S., Flagan, R.C., Seinfeld, J.H., 2007. Secondary organic aerosol formation from *m*-xylene, toluene, and benzene. Atmospheric Chemistry and Physics 7, 3909–3922.

Odum, J.R., Hoffmann, T., Bowman, F.M., Collins, D., Flagan, R.C., Seinfeld, J.H., 1996. Gas/particle partitioning and secondary organic aerosol yields. Environmental Science and Technology 30, 2580–2585.

Odum, J.R., Jungkamp, T.P.W., Griffin, R.J., Flagan, R.C., Seinfeld, J., 1997a. The atmospheric aerosol-forming potential of whole gasoline vapor. Science 276, 96–99.

Odum, J.R., Jungkamp, T.P.W., Griffin, R.J., Forstner, H.J.L., Flagan, R.C., Seinfeld, J.H., 1997b. Aromatics, reformulated gasoline, and atmospheric organic aerosol formation. Environmental Science and Technology 31, 1890–1897.

Olariu, R.I., 2001. Atmospheric Oxidation of Selected Aromatic Hydrocarbons, PhD thesis, University of Wuppertal, Germany.

Olariu, R.I., Barnes, I., Arsene, C., Becker, K.H., Wirtz, K., 2001. Studies on the atmospheric oxidation of phenol: II. Secondary organic aerosol formation. In: The European Photoreactor EUPHORE, 3rd Report 2000. Ed. Institute of Physical Chemistry, Bergische Universität Wuppertal, Germany, pp. 27–38.

Olariu, R.I., Klotz, B., Barnes, I., Becker, K.H., Mocanu, R., 2002. FT-IR study of the ring-retaining products from the reaction of OH radicals with phenol, *o*-, *m*-, and *p*-cresol. Atmospheric Environment 36, 3685–3697.

Olariu, R.I., Tomas, A., Barnes, I., Wirtz, K., 2003. Atmospheric ozone degradation reaction of 1,2-dihydroxybenzene: aerosol formation study. In: The European Photoreactor EUPHORE, fourth report 2001. Ed. Institute of Physical Chemistry, Bergische Universität Wuppertal, Germany, pp. 54–71.

Pankow, J.F., 1994a. An absorption model of gas/particles partitioning of organic compounds in the atmosphere. Atmospheric Environment 28, 185–188.

Pankow, J.F., 1994b. An absorption model of the gas/aerosol partitioning involved in the formation of secondary organic aerosol. Atmospheric Environment 28, 189–193.

Piccot, S.D., Watson, J.J., Jones, J.W., 1992. A global inventory of volatile organic compound emissions from anthropogenic sources. Journal of Geophysical Research 97, 9897–9912.

Seinfeld, J., Pandis, S.N., 1998. From Air Pollution to Climate Change. Atmospheric Chemistry and Physics. J. Wiley, New York.

Smith, D.F., Kleindienst, T.E., McIver, C.D., 1999. Primary product distributions from the reaction of OH with m-, p-xylene, 1,2,4- and 1,3,5- trimethylbenzene. Journal of Atmospheric Chemistry 34, 339–364.

Smith, D.F., McIver, C.D., Kleindienst, T.E., 1998. Primary product distribution from the reaction of hydroxyl radicals with toluene at ppb $NO_x$ mixing ratios. Journal of Atmospheric Chemistry 30, 209–228.

Song, C., Na, K., Cocker, D.R., 2005. Impact of the hydrocarbon to $NO_x$ ratio on secondary organic aerosol formation. Environmental Science and Technology 39, 3143–3149.

Song, C., Na, K., Warren, B., Malloy, Q., Cocker, D.R., 2007a. Secondary organic aerosol formation from m-xylene in the absence of $NO_x$. Environmental Science and Technology 41, 7409–7416.

Song, C., Na, K., Warren, B., Malloy, Q., Cocker, D.R., 2007b. Secondary organic aerosol formation from the photooxidation of p- and o-xylene. Environmental Science and Technology 41, 7403–7408.

Takekawa, H., Minoura, H., Yamazaki, S., 2003. Temperature dependence of secondary organic aerosol formation by photo-oxidation of hydrocarbons. Atmospheric Environment 37, 3413–3424.

Thüner, L.P., Bardini, P., Rea, G.J., Wenger, J.C., 2004. Kinetics of the gas-phase reactions of OH and $NO_3$ radicals with dimethylphenols. Journal of Physical Chemistry A 108, 11019–11025.

Tomas, A., Olariu, R.I., Barnes, I., Becker, K.H., 2003. Kinetics of the reaction of $O_3$ with selected benzenediols. International Journal of Chemical Kinetics 35, 223–230.

Volkamer, R., Jimenez, J.L., Dzepina, K., Salcedo, D., SanMartini, F.M., Molina, L.T., Worsnop, D.R., Molina, M.J., 2006. Secondary organic aerosol formation from anthropogenic air pollution: rapid and higher than expected. Geophysical Research Letters 33, L17811.

Volkamer, R., Uecker, J., Wirtz, K., Platt, U., 2002a. OH-radical initiated oxidation of BTXM: formation and atmospheric fate of phenol-type compounds in the presence of $NO_x$. In: Midgley, P.M., Reuther, M. (Eds.), Proceedings of the EUROTRAC-2 Symposium 2002. Margraf Verlag, Weikersheim, pp. 1–5.

Volkamer, R., Klotz, B., Barnes, I., Imamura, T., Wirtz, K., Washida, N., Becker, K.H., Platt, U., 2002b. OH-initiated oxidation of benzene; Part I. Phenol formation under atmospheric conditions. Physical Chemistry Chemical Physics 4, 1598–1610.

Weitkamp, E.A., Sage, A.M., Pierce, J.R., Donahue, N.M., Robinson, A.L., 2007. Organic aerosol formation from photochemical oxidation of diesel exhaust in a smog chamber. Environmental Science and Technology 41, 6969–6975.